UNIVERSITY OF TWENTE.

Bachelor thesis

Applied Physics

16th April 2013

Collapse of a sand bed

Author:
Christa Gjaltema

Supervisors:
Tess Homan
Prof. dr. Devaraj van der Meer

University of Twente

Physics of Fluids

The image was obtained at: http://www.featurepics.com/online/Sand-Grains-2085020.aspx

Abstract

Granular materials are widely used in industrial processes and the lack of understanding of the physics, specific for the behaviour of granular materials, makes it difficult, for example, to effectively design industrial facilities. This thesis takes a closer look at the behaviour of the compaction of a sand bed under different conditions; namely different ambient pressures and different shock strengths. This shock is achieved by releasing a ball from a specific distance and letting it swing against the side of a container filled with loosely packed sand.

The pressure difference above and below the sand and the drop of the sand bed were measured, and the maximum pressure reached during the experiments together with the behaviour of the decay of the pressure were analysed. The data shows that the compaction of the sand is very dependent on the release distance of the ball and thus the shock strength; the compaction is larger for larger deviations of the ball. Surprisingly it also depends on the ambient pressure inside the container, but to a lesser extent. It can be concluded that the compaction of the sand bed level both depends on the deviation of the ball and the ambient pressure inside the container.

Contents

Chapter 1

Introduction

Granular materials, such as sand, are very complex materials, they behave very differently from solids, liquids or gasses. A granular material can be considered as an additional state of matter because it can display both fluid-like and solid-like properties. One example is sand: Sand behaves like a solid when it is used in sand sculpture, is a liquid when looking at an hourglass and is in the gaseous state when in a sandstorm [6]. Because of the unique properties of granular materials, a lot of research has been done in this field, but granular materials are still very poorly understood [7].

Granular materials are widely used in industrial processes and the lack of knowledge of the physics that is specific for the behaviour of granular materials, makes it difficult, for example, to effectively design industrial facilities. A lot of research has gone into investigating the flow behaviour of granular materials [9], soil deformation during compacting [4], effect of gravity on the granular materials, which can be used to analyse the photos of planets [5], and so on. But still a lot of more research is needed to completely understand the behaviour of granular materials.

In this study the interaction between fine grains and the surrounding interstitial gas in a loosely filled granular bed is studied, during compaction. Earlier work by Royer *et al* at the university of Chicago [8] and Caballero *et al.* at the university of Twente [1], have confirmed the importance of the dynamic coupling between gas and granular motion. These research groups studied the formation of a granular jet which formed after dropping a solid sphere into a bed of loose fine sand. They discovered that, unlike the jet formed in fluid systems, the granular jet consist of two components. However the fluid jet models are of limited use for this more complex process involving the interaction between the sand an the interstitial air [8].

The research carried out at the University of Twente is similar to the research described in this thesis. A container filled with fine loose sand was used to study the behaviour of the compaction of a sand bed at atmospheric and lower pressures when an object is thrown against the side of the container. The theory and model used for the analysis of the data will be discussed in chapter 1. A more extensive description of the research and the results will follow in the theory, respectively chapter 3 and 4. This report will be wrapped up with a conclusion in chapter 5.

Chapter 2

Theory

In the experiments a container filled with very fine sand is used, which will be called a (porous) bed. The bed of a porous medium can be seen as a material with many capillary pores, which are parallel and run completely through the bed. The flow through such a porous medium is characterised with a constant, the permeability κ of the bed. The permeability is a measure of the ability of a porous medium to allow fluids to pass through it [10], i.e. the permeability is large when fluids can easily pass through the medium. In the first section an equation for the permeability will be introduced, and compared to measurements of the permeability of the bed in experiments prior to the experiments described in this report.

The change in the pressure difference after closing the air flow will be described next. This section will treat the theory of the pressure build up inside the system when air flows through a porous medium, and how this pressure build up will slowly go back to zero after the flow is stopped. In the last section a full model for the air flow and the pressure change inside the container, both as a function of time, will be treated. This al happens after the collapse of a loosely filled granular bed.

2.1 Permeability

In 1856 Darcy wrote a paper in which he introduced equation (2.1), now called Darcy's law. He found that the flow rate in a porous bed is proportional to the pressure drop over a given distance and inversely proportional to the viscosity of the fluid [10].

$$Q = -\frac{\kappa A}{\mu}\frac{\Delta P}{\Delta L}, \tag{2.1}$$

where Q is the flowrate in m^3/s, A the crossectional area in m^2, μ the dynamic viscosity of the fluid (Pa·s), ΔP the pressure drop (Pa) and ΔL is the length over which the pressure drop occurs (m).

After Darcy proposed his law, Kozeny developed a model for the permeability of porous medium which consists of a series of parallel capillaries. But since the capillary pores are in reality far from completely straight, the model had to be changed. After many adjustments, for example to account for the irregular path the flow takes through the medium, Carman came with a modified equation for the permeability [10]. This resulted in the Carman-Kozeny equation for the special container of uniform spheres [8]:

$$\kappa = \frac{d^2(1-\phi)^3}{180\phi^2}, \tag{2.2}$$

where κ is the permeability in m^2, d is the diameter of the grains (m) and ϕ is the packing fraction of the sand grains.

Before determining the permeabilities, it is important to explain the introduction of the packing fraction ϕ of a granular material in the previous formula. Most materials are highly irregular in shape and the results of a measurement can change if the particles are flipped or turned. So it is convenient to use a sphere with the same volume as the granular particles. For these spheres the packing fraction of the material can be calculated. The packing fraction is a measure of the volume occupied by granular particles, and is defined as the volume occupied by the solid phase divided by the total volume [2].

The sand used in the experiments consists of grains with a diameter between 20 and 60 μm with a packing fraction of 0.41. Inserting this into equation (2.2), yields a permeability which lies between $3.3 \cdot 10^{-12}$ and $3.0 \cdot 10^{-11}$ m^2. The permeability is mainly determined by the presence of the smallest grains in the sand and will therefore be closer to the lower value of the permeability. This was confirmed by an experiment, conducted at the University of Twente. In accordance with the latter, the permeability of the sand bed used in the experiments is $5{\cdot}10^{-12} \pm 1{\cdot}10^{-12}$ m^2 with no dependence on the bed height [3].

2.2 Flow through a porous bed

A schematic of the flow through the bed is shown in Figure 2.1. The air flows through two porous media before reaching the top of the container. The first is a porous plate (thickness H_p and permeability κ_p) which supports the sand and distributes the air evenly over the area, the second porous medium is the sand (thickness H_s and permeability κ_s).

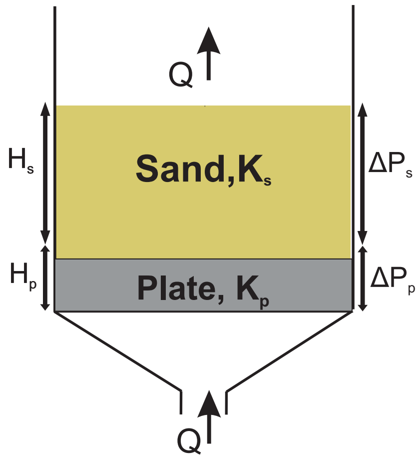

Figure 2.1: Schematic of the flow Q through the plate and the sand, with permeabilities κ_p and κ_s, respectively. Here H_p is the height (m) and ΔP_p the pressure difference (Pa) over the plate, H_s the height (m) and the ΔP_s the pressure difference (Pa) over the sand.

The flow rate in the two media can be calculated with Darcy's Law. The permeability of the plate should also be included, because the permeability is much smaller than that of the sand. This gives the following two equations for respectively the plate and the sand:

$$Q = -\frac{\kappa_p A}{\mu}\frac{\Delta P_p}{H_p}, \tag{2.3a}$$

$$Q = -\frac{\kappa_s A}{\mu}\frac{\Delta P_s}{H_s}. \tag{2.3b}$$

Because of the continuity equation (flow in = flow out) the total pressure difference below the

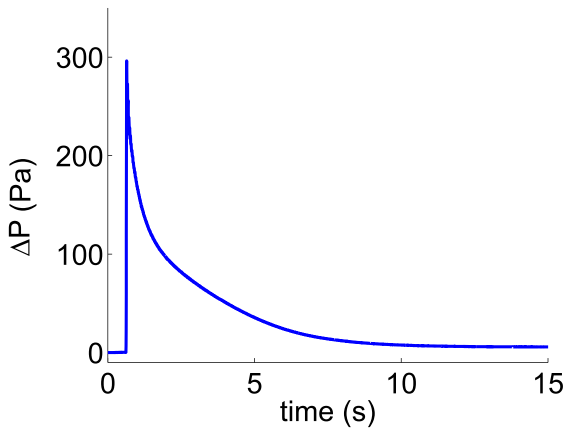

Figure 2.2: Example of the pressure difference decay in time, after the stop of the air flow through the sand.

plate and above the sand is:

$$\Delta P = \Delta P_p + \Delta P_s = -\frac{Q\mu H_p}{A\kappa_p} - \frac{Q\mu H_s}{A\kappa_s} = -\frac{Q\mu}{A}\left(\frac{H_P}{\kappa_p} + \frac{H_s}{\kappa_s}\right), \tag{2.4}$$

by rewriting equation (2.4) the flow Q becomes:

$$Q = \frac{\Delta P A\kappa_p\kappa_s}{\mu(H_s\kappa_p + H_p\kappa_s)}. \tag{2.5}$$

If the air flow is cut off, the pressure difference between the bottom of the plate and the top of the sand will go to zero after 10 to 30 seconds, depending on the ambient pressure in the container, an example of such a decay can be seen in figure 2.2. An equation for the decay can be derived with the use of Darcy's Law and the mass flow through the sand, the result of which can be seen in equation (2.6). The derivation of this equation can be found in appendix A.

$$\Delta P = \Delta P^* e^{-t/\tau}, \quad \text{with} \quad \frac{1}{\tau} = \frac{\kappa_p\kappa_s}{H_s\kappa_p + H_p\kappa_s}\frac{\rho_0 ART}{\mu V_1 M}, \tag{2.6}$$

with ΔP^* the initial pressure difference, τ the decay time, V_1 is the starting volume of the air above the sand (m^3), M the mass of the sand (kg), T is the temperature in K, ρ_0 is the density of air at constant pressure and temperature (kg/m^3) and R is the gas constant (J/mol·K) .

2.3 The model

In this section we will introduce the model, which describes the pressure inside, just above and below the sand and the pressure difference ΔP in time. This is after the sand collapses a distance H in this experiment, this is caused by the shock. The model is an 1D simplification of the pressures, thus the pressure differences in the y-direction are neglected. The starting pressure inside the container will be called the ambient pressure. The collapse will give rise to a pressure difference between the bottom and top of the sand. The pressure difference can be modelled with the diffusion equation[2].

$$\frac{d\Delta P}{dt} = D\frac{d^2\Delta P}{dx^2}, \quad \text{with} \quad D = \frac{\kappa P_0}{\mu(1-\phi)}, \tag{2.7}$$

with D the diffusion constant in m^2/s and P_0 the ambient pressure in Pa.

The bed drops a distance dH at time $t = 0$, where this drop is caused by, for example, a tap on the side of the container. The packing fraction of the sand will than change by $\Delta\phi$. The time scale of the compaction (<30ms) is much smaller than the diffusion time of air in a granular medium, but much larger than the time set by the speed of sound in air. This means the compaction process can be treated as isothermal ($PV = constant$). This will make it easier to determine the initial conditions in the next section.

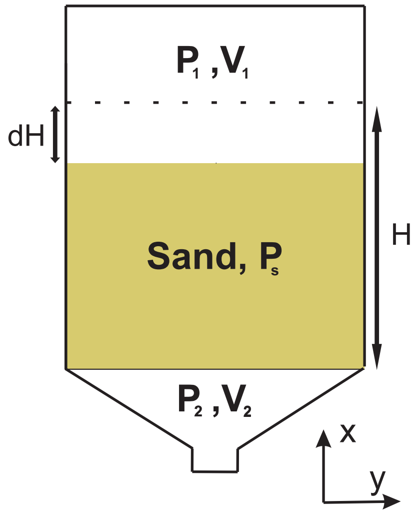

Figure 2.3: Schematic of the setup model, with dH the drop of the sand, H the starting height of the sand. P_1, V_1 and P_2, V_2 are respectively the pressure and volume above and below the sand, the pressure inside the sand is P_s.

2.3.1 Initial conditions

The initial pressure beneath the sand at the starting time is still equal to the ambient pressure. This is a result of the drop happening so fast that the air has no time to leave the sand. Thus the initial pressure difference is zero:

$$\Delta P_{2,i} = 0. \tag{2.8}$$

The pressure difference above the sand can be determined by using the fact that the compaction process is isothermal and very fast. The volume of air above the sand is V_1 and the sand drops a distance dH. Thus the new air volume is $V_1 + AdH$ and the initial pressure difference above the sand is:

$$\Delta P_{1,i} = \frac{P_0 V_1}{V_1 + AdH} - P_0, \tag{2.9}$$

with P_0 the ambient pressure in the container (Pa), A the cross-sectional area in m^2 and dH the drop of the sand in m.

Inside the sand it is a little more complicated since the packing fraction of the sand has to be taken into account. The packing fraction of the sand decreases but the volume occupied by the sand grains stays the same. The equation of the volume before and after the compaction can be seen below

$$\phi_0 AH = \phi_{after} A(H - dH). \tag{2.10}$$

From this expression the packing fraction ϕ_{after} after the collapse can be expressed in terms of ϕ_0,

$$\phi_{after} = \frac{\phi_0 H}{H - dH}. \tag{2.11}$$

The packing fraction is a number between the zero and one, thus the fraction of the interstitial air is equal to $1-\phi_0$. Again by using the fact that the process is isothermal the initial pressure difference inside the sand can be calculated:

$$P_0(1-\phi_0)AH = (\Delta P_{2,i} + P_0)(1-\phi_{after})A(H-dH), \tag{2.12}$$

which gives the following equation for the initial pressure difference inside the sand

$$\Delta P_{s,i} = \frac{P_0(1-\phi_0)H}{(H-dH)-\phi_0 H} - P_0. \tag{2.13}$$

An example of the initial conditions can be seen in figure 2.4.

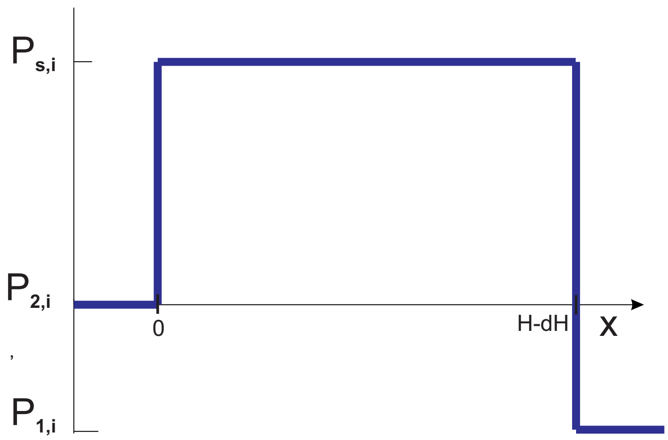

Figure 2.4: Example of the initial conditions inside the container in the x-direction. The pressure below x=0 corresponds with the starting pressure $P_{2,i}$, between the zero and $H-dH$ is the starting pressure inside the sand $P_{s,i}$ and for x larger than $H-dH$ is the pressure above the sand $P_{1,i}$.

2.3.2 Boundary conditions

The boundary conditions can be determined by using Darcy's law and the mass flow rate inside the system. There are two equations for the flow rate, at coordinate x. The first equation is the classic equation for the mass flow rate,

$$\frac{dm}{dt} = A\rho q\bigg|_x = A\rho\frac{\kappa}{\mu}\frac{dP}{dx}\bigg|_x, \tag{2.14}$$

with ρ the mass density of the substance in kg/m^3. The second equation for the mass flow rate is derived from the ideal gas law,

$$\frac{dm}{dt} = \frac{V}{RT}\frac{dP}{dt}, \tag{2.15}$$

with R the ideal gas constant (J/mol·K). By setting these two equations equal to each other and inserting the formula for the mass density, which can be simplified because ΔP is small,

$$\rho = \frac{P_0 + \Delta P}{RT} \approx \frac{P_0}{RT}, \tag{2.16}$$

into equation (2.14) will give the following two boundary conditions:

$$\frac{dP_1}{dt} = \frac{A}{V_1}\frac{\kappa P_0}{\mu}\frac{d\Delta P}{dx}\bigg|_{x=H-dH} \tag{2.17}$$

and

$$\frac{dP_2}{dt} = \frac{A}{V_2}\frac{\kappa P_0}{\mu}\frac{d\Delta P}{dx}\bigg|_{x=0}. \tag{2.18}$$

With these initial conditions and boundary conditions the model can simulate the pressure difference above and below the sand in time. The porous plate, with a permeability ten times smaller than the sand, is taken into consideration by adding a piece of porous material with a thickness H_p to the bed. An example of the pressure development can be seen in figure 2.5. The pressure difference below the sand starts at zero and rises slowly, and after it reaches a maximum the pressure difference goes back to zero, the equilibrium value. The pressure difference above the sand starts at the minimum value $\Delta P_{1,i}$ and returns slowly to the equilibrium.

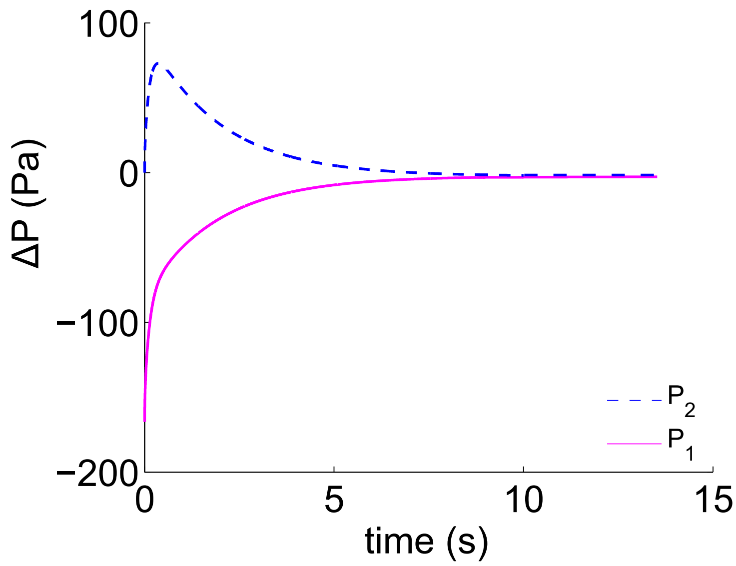

Figure 2.5: Example of the pressure difference above and below the sand as a function of time. The pressure above the sand, P_1 will start at at a pressure below zero, the pressure below the sand P_2 starts at zero and will rise.

Chapter 3

Experimental aspects

In this chapter the experiment will be discussed. This includes the experimental setup used for the measurements and its properties, and the preparation prior to these experiments. Measurements have been done for the height of a sand bed as a function of the deviation of a ball at normal pressure and for the height of the sand as a function of different ambient pressures.

3.1 Experimental setup

The setup used for the experiments can be seen in Figure 3.1. The sand in the setup contains grains of a diameter between the 20 and 60 μm and has a density of 2.21 ± 0.04 g/cm^3. The angle of repose for this material is 26°, if the sand is at an angle larger than the repose angle the sand will start to slide. The sand is poured into a container, made of perspex, with square sides of 14 cm and the sand bed has a depth of approximately 40 cm. The pouring of the sand will result in a packing fraction of 46%, however the packing fraction changes to 41% after fluidisation [1]. Fluidisation is the process of introducing an air flow to the bottom of the container. The sand will start to "boil" like water and after slowly closing the air flow the sand will settle in a looser packing compared to the starting situation.

The ball used as the impacting object is a steel ball with a diameter of 5 cm. The pressure difference below and above the sand is measured using two highly sensitive differential pressure sensors (Sensirion SPD2000-L) and the data is collected using LabView.

Because the setup will be used to measure the pressure above and below the sand and the height of the sand before and after the ball hits the side of the container, the setup must meet certain criteria:

- The contact time of the ball has to be small.
- No air can leave the setup during the experiment.
- The sand should drop as uniformly as possible.

The contact time of the ball has to be small for the energy has to be introduced to the system as fast as possible. Naturally the setup has to be airtight for measurements at ambient pressure (and at lower pressures) or else the pressure change during the drop of the sand can not be measured correctly. Also the height of the impact will have an influence on the drop of the sand, it is likely that the shock wave will be distributed more uniformly before it reaches the surface of the sand if the ball is placed very low. This will also be discussed in the next section.

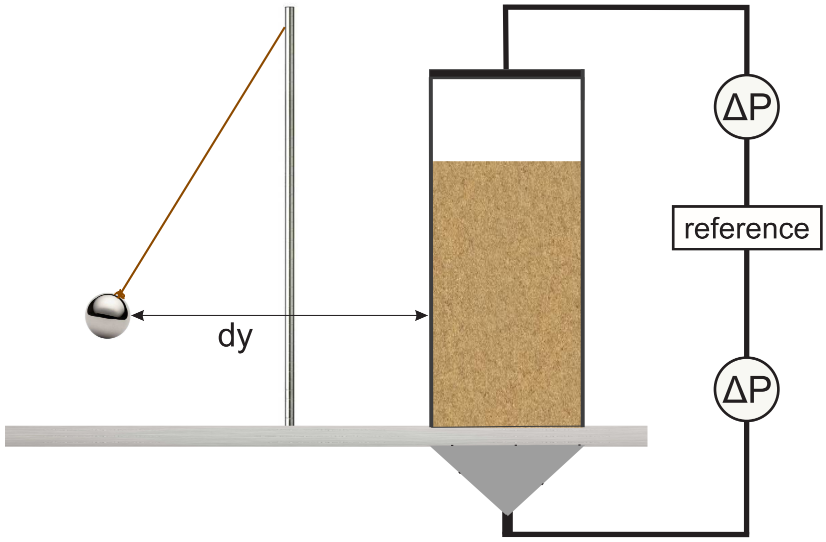

Figure 3.1: The setup used for the experiments. The ball is a distance *dy* away from the object. The container is filled with sand and the pressure is measured both in the top and bottom part of the setup with respect to a reference container that is initially brought to the same ambient pressure as the setup.

3.2 Execution

The first step was determining how to set up the experiment to meet up with the criteria. First a tennis ball filled with small copper balls was used as the impact object, however the contact time of the ball during impact was too long. The little copper balls also shifted during the impact, which made the impact irregular.This led to the conclusion that a solid ball was necessary. Next the optimal impact height of the ball had to be determined. Measurements were done for three different impact locations; at sand level, halfway the filling height of the sand and at the bottom of the container. It was concluded that the ball should make contact at the bottom. At this level the shock of the impact will distribute more evenly inside the sand before reaching the surface, thus the surface will drop more evenly. Also, the vibrations of the container will have less influence on the sand surface if the impact point is lower.

3.2.1 Atmosperic pressure

A series of experiments was done for different initial deviations of the ball at one atmosphere. The deviation ranged from 15 to 35 centimetres (dy, fig. 3.1) and the ball hit the surface at a height of 10.5 centimetres (center of the ball). A high speed camera was used to record the compaction of the sand bed and the movement of the ball, where the latter was used for the calculation of the speed of the ball at impact. The high speed camera has a Makro-Planar 1:2.8 lens with a focal length of 60 mm.

The sand has to be fluidised before the start of every experiment. First the valves connected to the setup and the top of de container should be open. Next an air flow was introduced to the sand. The sand will start to ”boil” like water. After a few seconds of fluidisation the air flow was gradually cut off and all the valves and the top were closed. The sand will settle, preferably every time at the same height, and the experiments can begin.

The pressure below and above the sand was measured for different deviations, simultaneously, the drop of the sand was recorded by a high speed camera. The measurements were triggered by a manual trigger, which was pressed when the ball was released. The analysis of the data and results will be discussed in the next chapter.

3.2.2 Lower pressures

In these experiments the pressure was lowered below one atmosphere, this was done using a vacuum pump. The container was brought to a maximum of 0.95 bar beneath atmospheric pressure. The vacuum pump draws out the air from below and above the sand. A complete vacuum can not be created for the setup, but for these experiment this will be sufficient.

The first step of the experiment was opening every valve and fluidising the sand by flowing air through the bottom of the container. Next, the valve connected to the outside had to be closed before turning on the vacuum pump. After slowly reaching the desired pressure the experiment could be continued at a reduced ambient pressure, of course after closing every valve.

Chapter 4

Results

This chapter will present the analysis of the high-speed movies of the compaction of the sand and the pressure difference inside the container. But first it is important to discuss the methods used for the analysis of the data, to get more insight in the process of the analysis.

4.1 The analysis

4.1.1 Sand surface

A Matlab program was written to analyse the videos which recorded the drop of the sand. The most important part of the analysis is the use of the Hough transform function in Matlab. The Hough function is used to detect linear lines in an image, which is used to determine the sand surface. It is also possible for this function to only detect lines arranged in a specific way. This orientation can range from $-90°$ to $90°$, with $-90°$ being the horizontal. In this container a range of $-90°$ to $-86°$ was used.

To make it easier for Matlab to determine the surface of the sand, the sand is centred and the casing and the ball are removed from the image with the use of a crop. Next a linear fit is used to determine the height of the Hough line, because it is possible that the Hough line does not start completely at the left of the image. The slope of the sand can change a bit during the drop, this means the starting point of the line could suddenly rise halfway the movie. This error is compensated by keeping the slope of the fit constant after the analysis of the first image. An example of the Hough line and its fit can be seen in figure 4.1, the program is quite accurate in determining the surface of the sand.

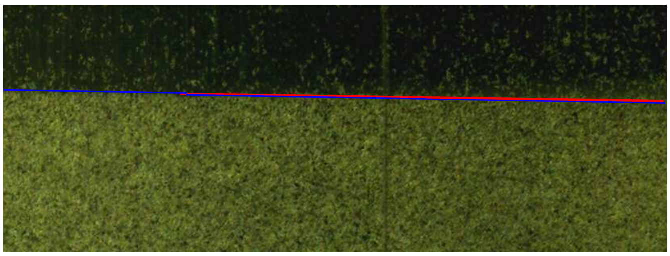

Figure 4.1: The sand surface determined by Matlab, with blue the linear fit and red the Hough line.

4.1.2 Impact speed

The speed of the ball at impact is also estimated with the use of Matlab and by recording the movement of the ball before and during impact with a high speed camera. The function *ginput* is used to determine the position of the ball in every image. This function makes it possible to determine the side of the ball by clicking on that position, *ginput* will then give the x- and y-value of that point. By doing this for every image of the recording and plotting the y-position against the time, the speed of the ball can be determined by calculating the slope of the plot. An example of such a plot can be seen in Figure 4.2.

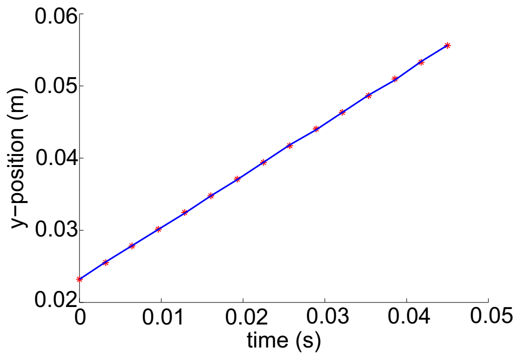

Figure 4.2: Plot of the y-position of the ball in time, with the endpoint the y-position of the ball just before it hits the container.

4.2 Atmospheric pressure

An example of the time evolution of the height of the the sand bed, for two different initial deviations of the ball, can be seen in Figure 4.3. Each colour represents three different measurements and the double analysis[1] with Matlab,. Figure 4.3(a) and figure 4.3(b) are the measurements of the drop with a deviation of 15 cm and 20 cm, respectively . It can be seen that, when the deviation is larger, the sand drops more, and the sand will also start to vibrate. Note that these vibrations are absent in figure 4.3(a). The different measurements match quite well, especially in the beginning of the measurement, thus the measurements are very reproducible.

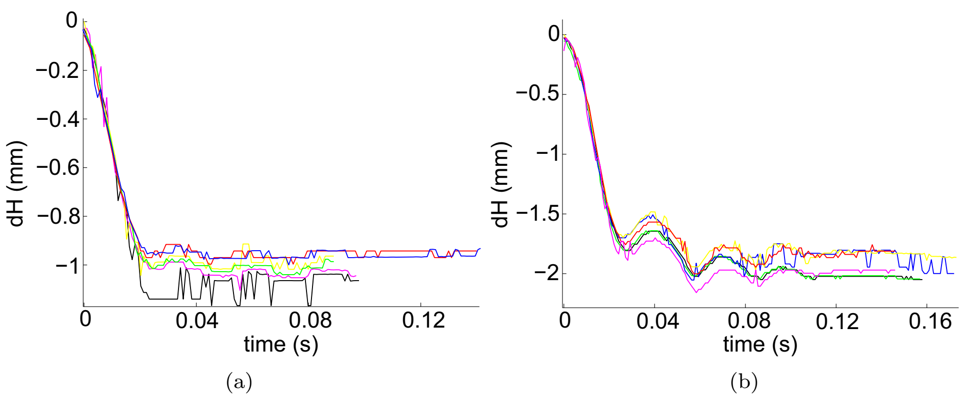

Figure 4.3: Measurements of the height of the drop dH of the sand bed during compaction for two different deviations of the ball (a) 15 cm and (b) 20 cm, the colours in the plot represent the different measurements.

[1]The three measurements were analysed twice in Matlab. This to minimize the possibility that Matlab did not determine the correct surface of the sand.

The previous two figures are only two of the seven measurements, that have been done for different deviations of the ball, ranging from 8 cm to 32 cm. The height of the drop dH of the sand as a function of the deviation can be seen in figure 4.4. The plot shows that the height of the drop of the sand bed is linear with the deviation of the ball and that the sand will drop more when the deviation is larger.

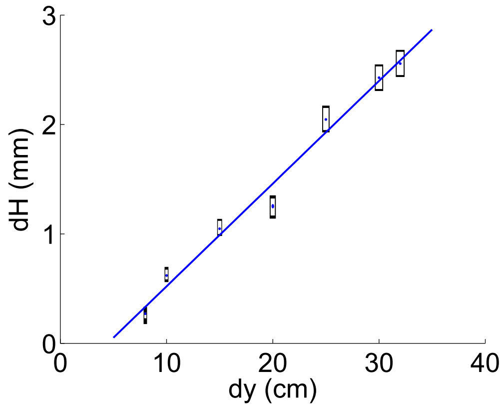

Figure 4.4: Maximum drop, dH, as a function of the deviation, dy, of the ball.

The time it takes for the height of the sand bed to drop to its final value and the collapse velocity of the sand were also analysed, the results of which can be seen in 4.5. The collapse velocity was estimated from the minimum slope of the dH versus the curves (see figure 4.3). The drop dH of the sand grows larger with a larger deviation, but the conditions remain the same, so it can be expected that the drop of the sand will take longer for larger deviations. This is confirmed in figure 4.5(a), unfortunately nothing can be said about the relation between the time and the deviation, because the data points are too widely spread. Fortunately the collapse velocity could be measured more accurately. The behaviour of the collapse velocity of the sand for different deviations can be seen in figure 4.5(b), this show a nice linear behaviour.

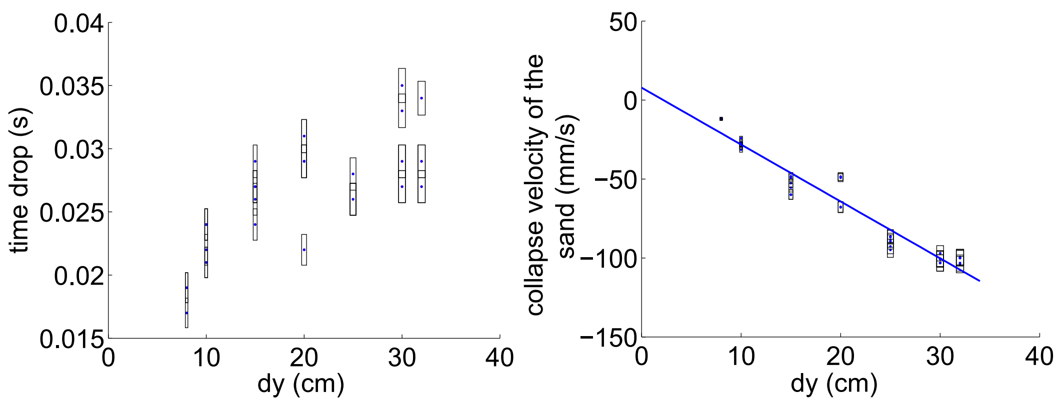

(a) (b)

Figure 4.5: Analysis of the data of the drop of the sand, with (a) the time it takes for the sand to drop to a minimum and (b) the speed of the drop of the sand for different deviations

The pressure difference inside the container, that is to say, above and below the sand bed, was also measured during the experiment. Five examples of these measurements can be seen in figure 4.6, each colour representing a different measurement. The five lines above the dotted line are the measurements below the sand. The pressure starts at zero and rises to a maximum, after which it goes to zero again. The lines below the dotted line are the measurements above the sand, these reach a minimum value very fast and subsequently slowly returns to zero pressure difference. Inside the figure is a close-up of the first second of the experiment. This shows that the pressure also vibrates for larger deviations, which is a result of the vibrations of the sand bed as a whole (see figure 4.3(a)). The decay of the pressure, both below and above the sand, is governed Darcy's law and can be fitted with an exponential. The fits are displayed as red dashed lines.

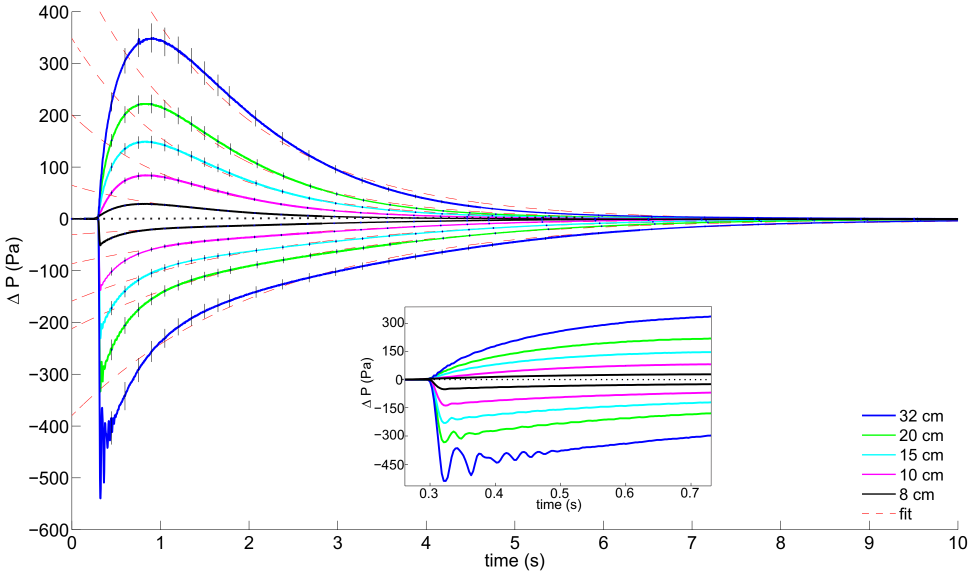

Figure 4.6: Pressure difference inside the container for different deviations of the ball, with the exponential fit, error margins and close up. The lines above the dotted line (at $\Delta P = 0$) are the pressure measurements below the sand bed, those below the dotted line are the measurements above the sand.

Figure 4.6 also shows that the maximum absolute pressure difference is larger for larger deviations. This is a result of a larger heigth of the drop of the sand, i.e. a larger volume increase above the sand. These maximum pressure differences are plotted in figure 4.7(a) and show a linear relation with the drop of the sand. The inverse decay constants $1/\tau$ were also calculated and are shown in figure 4.7(b), they do not fluctuate significantly.This was expected because the decay time τ does not depend on the height of the drop of the sand dH, see equation (2.6).

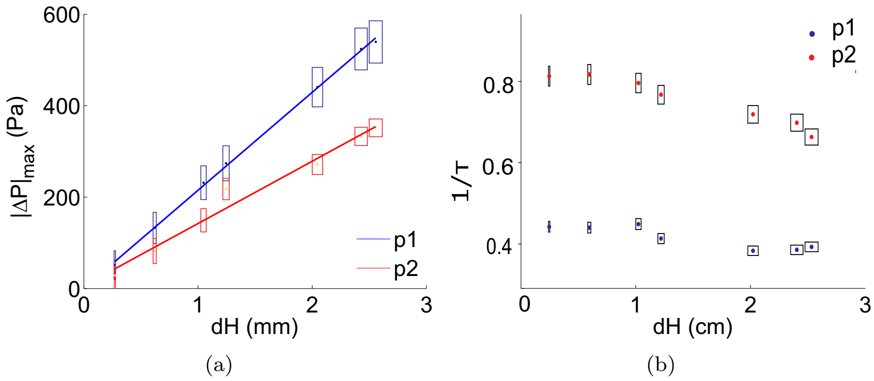

(a) (b)

Figure 4.7: Analysis of the data of the pressure differences, with (a) the absolute maximum pressure difference reached during the experiments and (b) the inverse decay time $1/\tau$ as a function of the drop dH, below and above the sand. Here the blue error boxes and the blue linear fit correspond to the upper part of the setup, i.e. above the sand bed (p1), whereas the red ones pertain to the lower part of the setup, below the sand bed and the porous plate.

4.3 Lower pressures

In this part of the research the pressure inside the container, the ambient pressure P_0, is varied while the deviation of the ball is held at a constant distance of 29 cm. After the fluidization procedure the air is slowly removed from the container, if this happens slowly enough the packing fraction of the sand will not change and the conditions will remain the same. First the height of the drop of the sand bed for different pressures is measured, the results of which can be seen in figure 4.8. The height of the drop is smaller for smaller pressures and the change in the height of the drop is much smaller compared to the maximum height of the drop when varying the deviation of the ball.

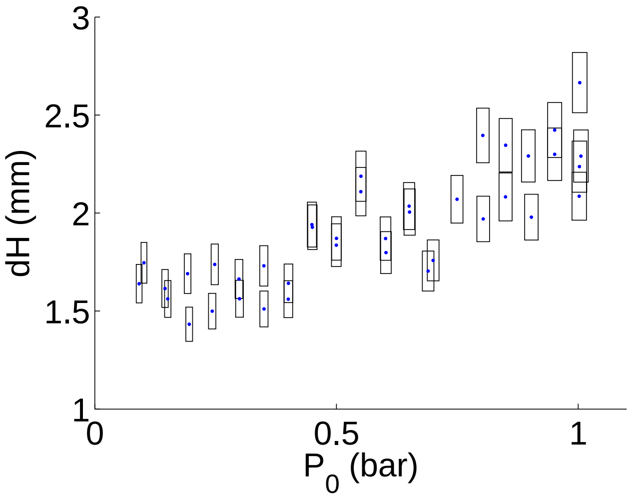

Figure 4.8: The maximum drop of the sand, dH, as a function of the ambient pressure, P_0, inside the container. The deviation of the impacting ball has been fixed to the constant value of 29 cm.

When taking a look at the collapse velocity of the sand in figure 4.9(b), it can be concluded that the speed of collapse does not change significantly for lower pressures. Also the time the bed takes to reacht the compact state is almost constant for different ambient pressures, as can be seen in figure 4.9(a). Thus the collapsing process does not change significantly when the ambient pressure is varied.

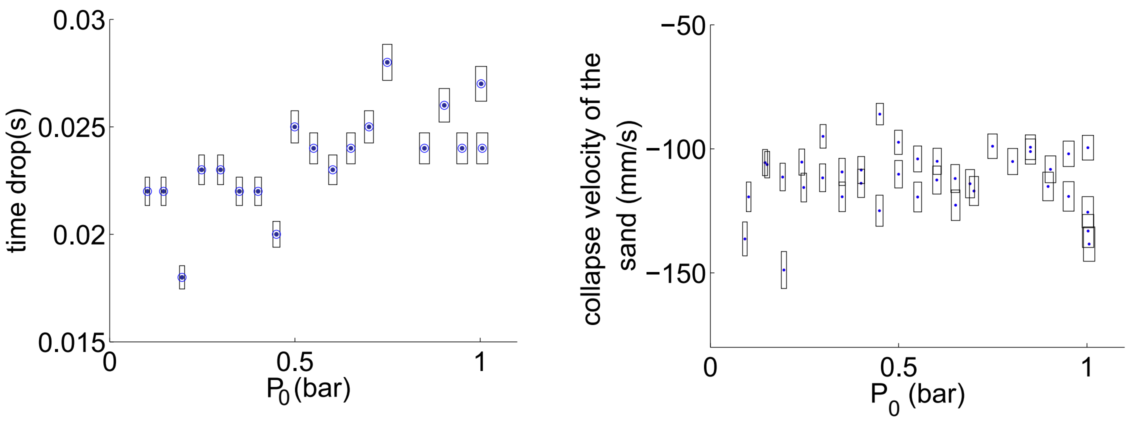

Figure 4.9: Analysis of the data of the drop of the sand, with (a) the time the drop of the sand takes and (b) the collapse velocity of the sand as a function of the ambient pressure P_0.

The pressure difference inside the container was also measured during these experiments, the results of which are shown in figure 4.10. The lines above the dotted line at zero pressure difference are the measurements below the sand, the lines below the dotted line are the measurements above the sand. The vibrations of the container and the sand are again visible in the close up. However in this experiment the vibrations are smaller when the pressure is lowered, probably because there is less air available to vibrate. These measurements are very similar to the pressure measurement in the previous section, but there is one difference which is easily spotted; the decay time τ of the exponential is different.

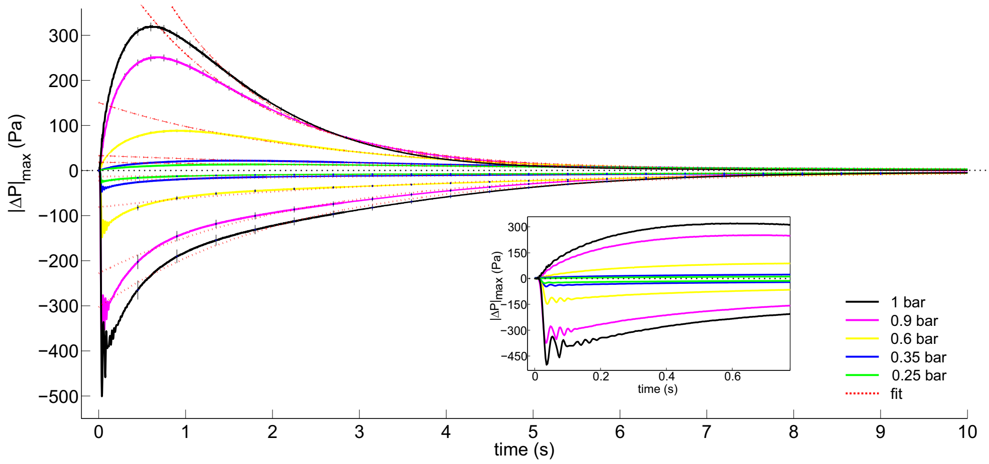

Figure 4.10: Pressure difference inside the container for different ambient pressures inside the container, with the exponential fit, error margins and close up. The lines above the dotted line (at $\Delta P = 0$) are the pressure measurements below the sand, below the dotted line are the measurements above the sand.

That the decay time τ is different can be seen in figure 4.11(b), where it is observed that $1/\tau$ is larger at higher ambient pressures. This can be explained with equation (2.6), in which $1/\tau$ is found to be linear with the ambient pressure, which is confirmed in figure 4.11(b). The behaviour of the maximum pressure difference is also different than in the previous section. Figure 4.11(a) shows that the maximum pressure difference is an exponential function $(a * exp(b * x) + c)$. If the drop of the sand did not change for different pressures, the data would have shown a linear dependence. But since the drop does change, this behaviour will be different. Also the maximum pressure difference goes to zero for lower pressures, because the amount of air in the system will also decrease.

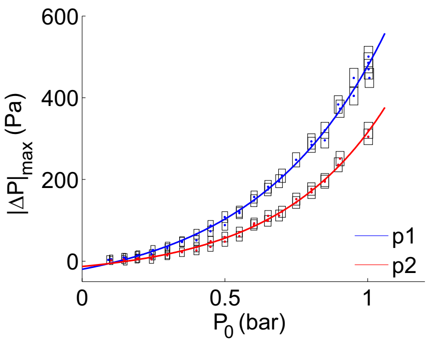

(a)

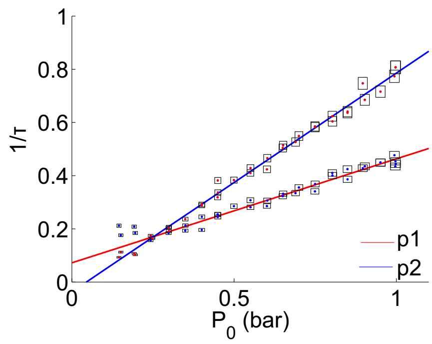

(b)

Figure 4.11: Analysis of the data of the pressure measurements, with (a) the absolute maximum pressure difference reached during the experiments and (b) the inverse decay time 1τ as a function of the ambient pressure P_0, below and above the sand. Blue corresponds to the upper and red to the lower part of the setup.

4.4 Final result

Ideally the results of all the pressure measurements would collapse into two single pressure lines (above and below the sand) when the data is non-dimensionalized. The pressure can be made dimensionless by multiplying it with $H/(P_0 dH)$, the time will be non-dimensionalized when multiplying it with $\kappa P_0/H^2\mu(1-\phi)$. The end result is shown in figure 4.12. The data does indeed collapse quite nicely into two lines. The two lines contain the data of the two different experiments. The orange lines are the pressures below the sand, the blue lines are the pressures above the sand. The collapsed lines of the simulated data of the model are also included in this figure, these are the purple dotted lines. The shape of these two lines looks very similar to the experimental data, the only difference is the maximum pressure below the sand, which is much larger than the experimental data.

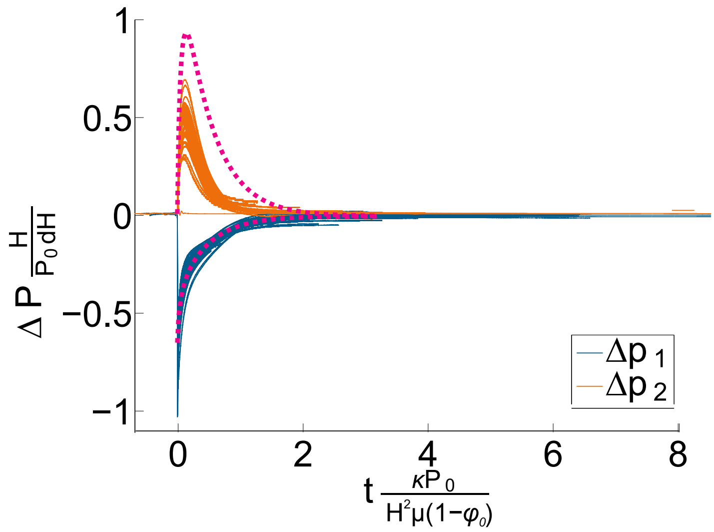

Figure 4.12: The non-dimensionalized pressure differences inside the container for different deviations and different ambient pressures. The blue and the orange lines are the measured pressure differences inside the container, the two purple lines are the pressure differences calculated by the model.

Chapter 5

Discussion and conclusion

When a ball is impacted against the side of a container which contains loosely packed sand at ambient pressure, the sand level will drop over a distance dH. This height of the drop will be larger when the ball is released from a larger distance and will grow linearly with a larger release distance. It is plausible that the height of the drop will reach a maximum, thus that the height of the drop will stop growing beyond a certain threshold deviation. This maximum was however not explored, because the container could not handle larger impacts of the ball. Also it would be interesting to research the height of the drop of the sand for different initial packing fractions.

The collapse velocity of the sand shows a nice linear behaviour as a function of the deviation of the ball, which is in correspondence with the linear behaviour of the height of the drop of the sand bed for different deviations.

During these experiments the pressure difference above and below the sand was also measured. This behaviour corresponds nicely with the pressure profile predicted by the model. The maximum pressure difference also shows a nice linear behaviour for different drops, as expected from the model. The inverse decay constant $1/\tau$ shows no dependence on the drop of the sand, which agrees with the theory; the equation for the decay constant does not depend on the magnitude of the height drop.

After these experiments the ambient pressure inside the container was varied while the deviation of the ball was held constant. It was expected that the height of the drop would be constant for different pressures and that the height of the drop would depend primarily on the magnitude of the shock against the container. But the data shows that the drop becomes somewhat smaller for smaller ambient pressures, thus indicating that the height of the drop does depend on the ambient pressure. However, it is still unclear why this happens. Further experiments are required to understand this behaviour.

As in the previous experiments, the pressure difference above and below the sand was also measured. The decay constant is linear with the ambient pressure, which is expected from the theory, which stated that the decay constant is inversely proportional with the ambient pressure.

But the most important result is the collapse of all the pressure difference data. The data for all different deviations and all different ambient pressures collapses into a single line, when non-dimenionsonliazed. The shape of this line corresponds to that of the line predicted by the model. The final conclusion that the height of the drop of the sand bed is not only dependent on the force of the impact, but also, surprisingly, dependent on the ambient pressure inside the container.

Bibliography

[1] Gabriel Caballero, Raymond Bergmann, Devaraj van der Meer, Andrea Prosperetti, and Detlef Lohse. Role of air in granular jet formation. *Physical Review Letters*, 99, 2007.

[2] Richard Holdich. *Fundamentals of Particle Technology*. Midland Information Technology and Publishing.

[3] Tess Homan. The effect of air on sand near the jamming point. Master's thesis, University of Twente, 2009.

[4] T. Kellera, M. Lamandc, S. Pethd, M. Berlif, J.-Y. Delenneg, W. Baumgartend, W. Rabbelh, F. Radjag, J. Rajchenbach, A.P.S. Selvaduraij, and D. Ork. An interdisciplinary approach towards improved understanding of soil deformation during compaction. *Soil and Tillage Research*, 128:61 – 80, 2013.

[5] N. Murdoch, B. Rozitis, K. Nordstrom, S. F. Green, P. Michel, T.-L. de Lophem, , and W. Losert. Granular convection in microgravity. *Physical Review Letters*, 110:1, 2013.

[6] Sidney R. Nagel, Robert P. Behringer, and Heinrich M. Jaeger. The physics of granular materials. *Physics Today*, 49:32, 1996.

[7] Patrick Richard, Mario Nicodemi, Renaud Delannay, Philippe Ribire, and Daniel Bideau. Slow relaxation and compaction of granular systems. *Nature Materials*, 4:121 – 128, 2005.

[8] John R. Royer, Eric I. Corwin, Andrew Flior, Maria-Luisa Cordero, Mark L. River, Peter J. Eng, and Heinrich M. Jaeger. Formation of granular jets observed by high-speed x-ray radiography. *Nature Physics*, 1:164 – 167, 2005.

[9] Chris H. Rycroft. Research granular materials.

[10] R. Rhodes Trussell and Melissa Chang. Review of flow through porous media as applied to head loss in water filters. *Environmental Engineering*, 125:998 – 1006, 1999.

Appendix A

Decay of the pressure difference

In this appendix the equation for the decay of the pressure difference will be derived, with the use of Darcy's law and the mass flow through the sand. A schematic of the setup used for the calculations can be seen in figure A.1.

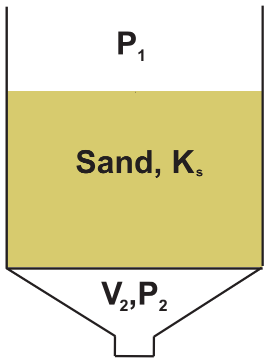

Figure A.1: The setup used in the experiments. The bottom of the container is closed and there is a pressure difference ΔP between P_2 and P_1. Below the sand is a volume V_2 of air at a pressure $P_2 = P_1 + \Delta P$ that slowly flows through the sand bed. The top of the container is left open, and $P_1 = P_0$ (1 bar).

The flow rate of the air was already calculated in chapter 2, the result is,

$$Q = \frac{\Delta P A \kappa_p \kappa_s}{\mu(H_s \kappa_p + H_p \kappa_s)}. \tag{A.1}$$

The mass flow of the air through the sand is equal to the density of the air ρ_0 in kg/m^3 (at constant pressure and temperature) times the flow rate, with the flow rate from equation (A.1):

$$\frac{dm}{dt} = \rho_0 Q = \frac{\rho_0 \Delta P A \kappa_p \kappa_s}{\mu(H_s \kappa_p + H_p \kappa_s)}. \tag{A.2}$$

The pressure below the setup is $P_2 = P_1 + \Delta P$, the following equation is obtained by inserting the pressure in the ideal gas law $PV = nRT$, with $n = m/M$:

$$(P_1 + \Delta P)V_2 = \frac{mRT_0}{M}, \tag{A.3}$$

with n the number of moles gas, m the mass of the air (kg) and M the molar mass of the air (kg/mol), T_0 the temperature (K) and R the gas constant (J/K·mol).

By differentiating equation (A.3) with respect to time, the pressure above the sand, P_1, will disappear from the equation because it is a constant. This will give the following equation,

$$\frac{d\Delta P}{dt}V_2 = \frac{dm}{dt}\frac{RT_0}{M}. \tag{A.4}$$

Thus a second equation for the mass flow can be determined:

$$\frac{dm}{dt} = \frac{d\Delta P}{dt}\frac{V_2 M}{RT_0} \tag{A.5}$$

Setting these two equations, (A.2) and (A.5), equal will give the following equation:

$$\frac{dm}{dt} = \frac{\rho_0 \Delta P A \kappa_p \kappa_s}{\mu(H_s\kappa_p + H_p\kappa_s)} = \frac{d\Delta P}{dt}\frac{V_2 M}{RT_0}. \tag{A.6}$$

Rewriting equation (A.6) will give the following differential equation:

$$\frac{d\Delta P}{\Delta P} = -\frac{\kappa_p\kappa_s}{(H_s\kappa_p + H_p\kappa_s)}\frac{\rho_0 A R T_0}{\mu V_2 M}dt \tag{A.7}$$

The solution of the differential equation is:

$$\Delta P = \Delta P^* e^{-t/\tau}, \quad \text{with} \quad \frac{1}{\tau} = \frac{\kappa_p\kappa_s}{H_s\kappa_p + H_p\kappa_s}\frac{\rho_0 A R T}{\mu V_2 M} \tag{A.8}$$

With ΔP^* the initial pressure difference and τ the decay time of the equation.